APL Materials

RESEARCH ARTICLE | MAY 14 2024

Non-conventional resonant behavior of an unconfined magnetic domain wall in a permalloy strip

Laura Fernández-García ; Sandra Ruiz-Gómez ; Rubén Guerrero ; Rodrigo Guedas ; Claudio Aroca ; Lucas Perez ; José L. Prieto ; Manuel Muñoz

APL Mater. 12, 051116 (2024)
https://doi.org/10.1063/5.0206170

Non-conventional resonant behavior of an unconfined magnetic domain wall in a permalloy strip

Cite as: APL Mater. 12, 051116 (2024); doi: 10.1063/5.0206170
Submitted: 29 February 2024 • Accepted: 29 April 2024 •
Published Online: 14 May 2024

Laura Fernández-García,[1] Sandra Ruiz-Gómez,[2,a)] Rubén Guerrero,[3] Rodrigo Guedas,[4,b)] Claudio Aroca,[4] Lucas Perez,[5] José L. Prieto,[4] and Manuel Muñoz[1,c)]

AFFILIATIONS

[1] Instituto de Tecnologías Físicas y de la Información ITEFI-CSIC, Madrid 28006, Spain
[2] Max Planck Institute for Chemical Physics of Solids, Dresden 01187, Germany
[3] Instituto Madrileño de Estudios Avanzados–IMDEA Nanociencia, C/Faraday 9, Madrid 28049, Spain
[4] Instituto de Sistemas Optoelectrónicos y Microtecnología–Universidad Politécnica de Madrid (ISOM-UPM), Madrid 28040, Spain
[5] Dpto. Física de Materiales, Universidad Complutense de Madrid, Madrid 28040, Spain

[a)] **Current address**: Alba Synchrotron Light Facility, Barcelona, Spain.
[b)] **Current address**: Univ. Grenoble Alpes, CNRS, CEA, Grenoble INP, SPINTEC, 38000 Grenoble, France.
[c)] **Author to whom correspondence should be addressed:** manuel.munoz@csic.es

ABSTRACT

The resonant dynamic of a magnetic domain wall in a permalloy microstrip has been investigated using an innovative experimental setup that enables a simultaneous measurement of the ferromagnetic resonance and the magnetoresistance. The resonance frequency associated with the presence of the magnetic domain wall increases linearly with the external magnetic field in the range of fields where the domain wall is present in the microstrip. This linear behavior is unusual in a domain wall and not related to the standard resonant modes of a magnetic domain wall, such as breathing, twisting, or translational modes. The slope of this linear dependency is 1.38 GHz/mT, which is an incredibly large value and allows the detection of very small changes in the external magnetic field. This linear behavior opens a path for developing a highly tunable radio frequency oscillator or a magnetic sensing device where the presence of an external field is detected via small variations in the resonant frequency of the domain wall.

I. INTRODUCTION

Magnetic domain walls (DWs) represent stable configurations of magnetization that have attracted significant attention in recent years, owing to both their fundamental properties and their potential application in spintronic devices, such as data storage, logic devices,[1,2] and magnonic devices.[3] The dynamic response of a DW to an external input (a magnetic field or electric current) is of particular interest. Early works showed that radio frequency (RF) excitation led to a decrease in the DW depinning field,[4] an enhancement of the DW nucleation field,[5] or it could even be used to determine the mass of the DW.[6,7] The frequency response of the DW has also been used to assist in the depinning of an adjacent DW,[8] as a broadband spin wave and elastic wave emitter,[9] or to guide spin waves.[10] Arguably, though, the main goal of this topic is the implementation of a domain wall oscillator where the response in the frequency of the DW is used to realize a highly tunable RF oscillator. There have been several proposals for domain wall oscillators,[11–15] mostly based on the results of micromagnetic simulations rather than on experimental demonstrations. Nevertheless, there are very relevant experimental characterizations of the resonant behavior of a single DW. Sandweg *et al.*,[16] using Brillouin light scattering, characterized the frequency response of a DW pinned in an antinotch of a circular nanostrip. They found that the resonant frequency associated with the DW decreased as the depinning field approached. Lepadatu *et al.*[17,18] electrically characterized the resonant behavior

of a DW in a permalloy strip pinned at a very deep notch. The characteristic frequency of this pinned DW was roughly constant (slightly decreasing) with the increasing current density. A DW resonant frequency that is constant with the increasing external field (or current density) is typical of a pinned DW. The three main resonant modes of a pinned DW, namely the "breathing," "twisting," and "translational" modes, all have a characteristic constant resonant frequency when the field (or current) is much smaller than the depinning field (or current).[19,20] Then, as the field (current) gets closer to the depinning field (current), the DW characteristic frequency decreases.

On the other hand, from a fundamental and application point of view, it would be interesting to have a characteristic resonant behavior where the frequency increases linearly with the external magnetic field (or current), so the device can be easily tuned. Bedau *et al.*,[21] by measuring the dependence of the depinning field with the frequency of the electric current, indirectly measured the resonant frequency of a geometrically confined vortex wall but not in the vicinity of a notch or a strong pinning point. They found that the resonant frequency of the vortex slightly increased with the external magnetic field at a rate of 50 MHz/mT, which resembles the behavior of a vortex core orbiting around a central point,[22,23] and it is clearly different from the quasi-constant resonant frequency of the pinned DW. This result indicated that a linear increase in the resonance frequency of a DW may be found if the DW is unconstrained in a weak pinning regime.

In this work, we report a detailed spectral characterization of a non-confined DW in a very weak pinning regime. In a 10 μm wide permalloy strip, we serendipitously found a very large transversal-like DW, weakly pinned at the nanoscopic structure of the strip. The shape of this DW is surprisingly repeatable, regardless of the number of times the external field is cycled. In these conditions, using an innovative dual transport set-up that measures the frequency response of the DW and its characteristic anisotropic magnetoresistance (AMR), we fully characterized the resonant behavior of this weakly pinned DW up to its depinning field at 0.8 mT. We found that the resonance frequency of this DW increases with the external magnetic field with perfect linearity at a striking rate of 1.38 GHz/mT. This finding opens the door to engineering similar devices that are easily tunable, where, in the presence of a bias field and with appropriate field compensation, the frequency response of the system would allow the detection of tiny variations of the external magnetic field.

II. FABRICATION AND METHODOLOGY

In this study, we have used an innovative setup to measure simultaneously the ferromagnetic resonance (FMR) and AMR of the magnetic DW in microstrips.

The microstrips (10 μm wide and 100 μm long) were fabricated using electron beam lithography, DC magnetron sputtering, and lift-off on Si/SiO_2 substrates. The metallic structure consists of Cr (1 nm)/$Ni_{80}Fe_{20}$ (20 nm)/Au (4 nm). Subsequently, the microantenna and contacts were also deposited via DC sputtering directly on top of the microstrip with the structure (1 nm Cr/50 nm Au).

The essential elements of the set-up are depicted in Fig. 1. To measure the FMR, a microwave signal of constant power of 0 dBm, generated by an MGX N5282A Vector Signal Generator, is applied in the RF port of a T bias connected to the microantenna. This RF signal induces a radio frequency magnetic field (h_{RF}) perpendicular to the long axis of the microstrip. The reflected power is detected with a Schottky diode (KEYSIGHT 8473B.)To achieve high sensitivity and precision, a field modulation and a lock-in amplifier were used to obtain the derivative of the reflected power vs the static external magnetic field, applied parallel to the long axis of the microstrip.

To detect the presence of a DW in the microstrip, a setup to measure the AMR of the DW is connected to the DC port of the T-bias. When a DW nucleates, there is a change in the electrical

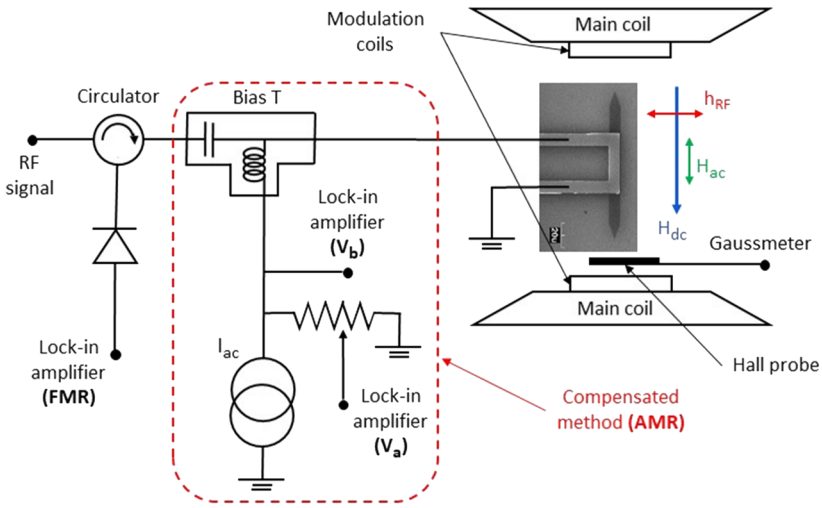

FIG. 1. Schematics of the experimental set-up for the simultaneous measurement of ferromagnetic resonance and magnetoresistance. The part of the set-up dedicated to measuring AMR by the compensated method is marked by a red square.

resistance of the device due to the AMR of the magnetic microstrip.[24,25] To detect this very small change, we use a lock-in technique, the so called compensated method.[26] In this method, the resistance of the device is compared with the resistance of a load connected in parallel to the sample. An alternating electric current is supplied by a 6221 Keithley source to the device and the load. The resistance of the reference load is adjusted to a value close to the resistance of the device at magnetic saturation (without a DW in the microstrip). A 7280 Perkin Elmer digital signal processing lock-in amplifier is used to compare the voltage drop between the variable reference load and the sample while sweeping the static magnetic field.

III. RESULTS

We performed FMR measurements within the frequency range of 2.0 to 3.5 GHz. Figure 2(a) shows FMR reflection as the static applied field is swept from −10 to 10 mT. In these measurements, two relatively broad peaks can be observed (for both directions of the static magnetic field), and their position varies depending on the frequency of the RF signal applied to the micro-antenna. Figure 2(b) presents the measurements for the whole range of frequencies measured. We can observe that these two peaks shift toward higher H_0 values with increasing h_{RF} frequency, following the square root behavior expected from Kittel's equation for the FMR of thin films. Such behavior indicates that these wideband resonances measured for negative and positive H_{dc} fields correspond to the resonance of the microstrip, with the magnetization pointing toward negative and positive directions, respectively.

Regarding the narrowband peak visible close to zero external field, it is observed only in the range of h_{RF} from 2.0 to 2.8 GHz. Its characteristic H_0 is much smaller than the one for the broadband peaks and limited to values between 0.3 and 1.0 mT. In addition, in contrast to the behavior of the strip resonances that follow Kittel's equation, their evolution shows a linear dependence on the h_{RF} frequency. Moreover, this specific narrowband resonance was observed exclusively in experiments that involved a reversal in the direction of the static magnetic field. Under this condition, the magnetization switches between initial and final states, and the peak appears in the same range of fields that allows the nucleation of the DW in the microstrip. This led us to think that these narrowband peaks could have their origin in the presence of a DW.

To verify the presence of the DW, we performed both magneto-optical Kerr effect (MOKE) microscopy and magnetotransport measurements. In Fig. 3(a), we show a MOKE image at 1 mT after saturating the sample in the negative direction parallel to the strip, where the characteristic contrast of two domains, separated by a DW, is visible. To correlate the narrowband peak with the presence of a DW, we carried out simultaneous AMR measurements and RF characterization from negative to positive magnetic saturation.

The profile of the change in the resistance of the microstrip, obtained with the experimental setup explained earlier, is represented in Fig. 3(b). This resistance profile (red curve) shows a gradual decrease in the resistance for positive low H_{dc} fields, characteristic of experiments in which a DW is injected into the strip.[26]

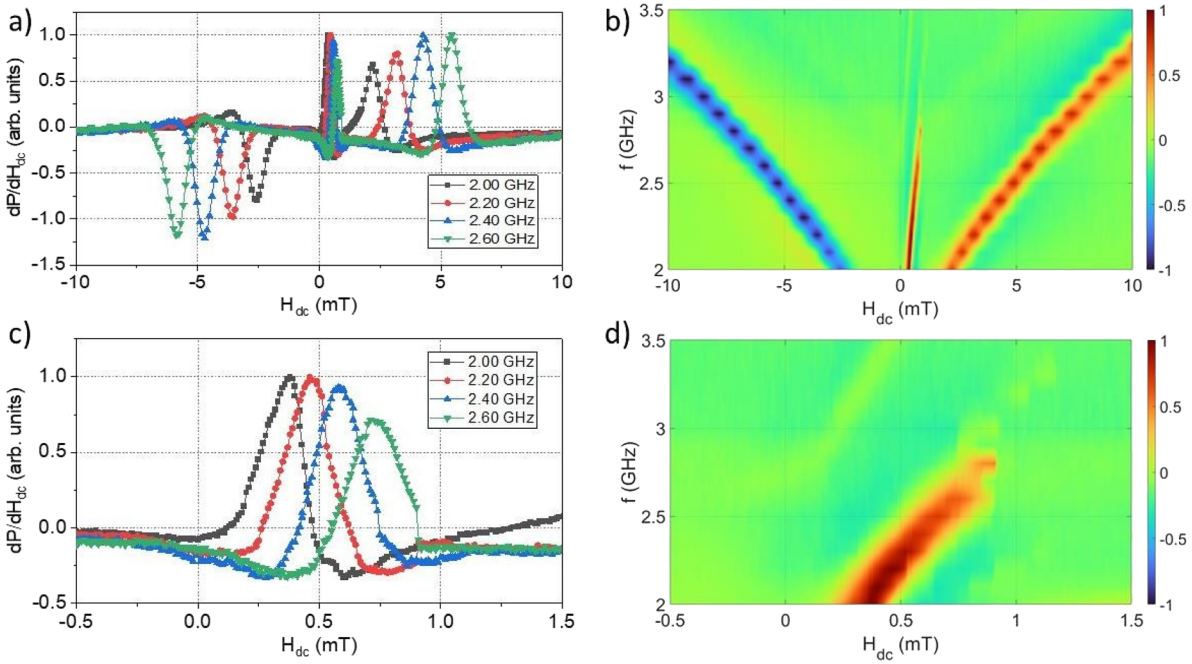

FIG. 2. Ferromagnetic resonance (FMR) curves, measured as the derivative of the reflected power by the device, as a function of the applied static magnetic field (H_{dc}). (a) Selected normalized curves of the FRM for different h_{RF} frequencies. (b) Normalized intensity of the FMR for h_{RF} frequencies from 2.00 to 3.50 GHz in steps of 0.10 GHz. (c) and (d) are enlarged images from −0.5 to 1.5 mT of panel (a) and (b), respectively.

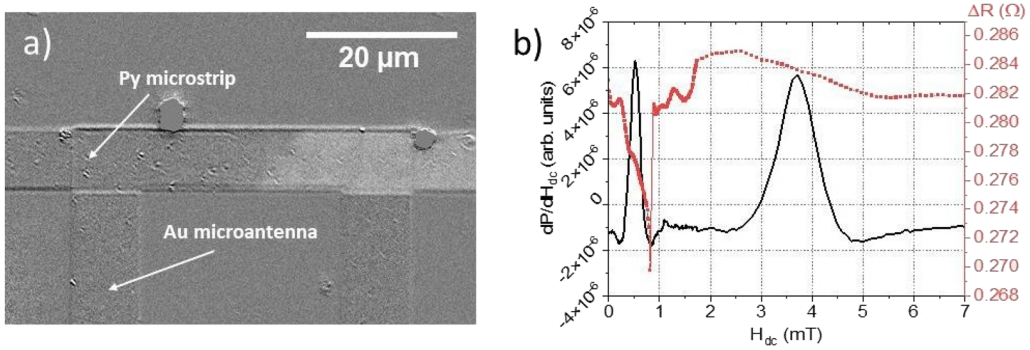

FIG. 3. (a) MOKE image of the microstrip measured for an applied magnetic field of 1 mT after saturating in the opposite direction. (b) Two independent measurements from 0 to 7 mT: black, FMR signal at 2.4 GHz; red represent a measurement of the change in the electrical resistance of the microstrip.

After the sharp increase in resistance, the DW has been depinned, and it is outside the area of measurement. As shown in the independent measurements in Fig. 3(b), the narrowband peak is simultaneous with the drop of AMR that marks the presence of the DW, and it vanishes in the sharp increase of resistance when the DW propagates toward the end of the strip.

Both MOKE imaging and AMR measurements confirm that a DW is present in the microstrip for positive values of the H_{dc} field near 1 mT, after a saturation in the negative direction.

In Fig. 4, the simultaneous FMR-AMR measurement was performed and represented in a narrow range of H_{dc} fields, from −0.5 to 2 mT, and for different h_{RF} frequencies. A shift of the center of the resonance peak (line) toward higher values is observed with increasing h_{RF} frequency. The AMR measurements, represented as lines and symbols, show an initial gradual decrease, starting at 0 to ∼1 mT, with a sharp increase marking the depinning and propagation of the DW.

In Fig. 4, the DW is detected by AMR measurements for all the h_{RF} frequencies. For 2.10 and 2.30 GHz, the H_{dc} interval in

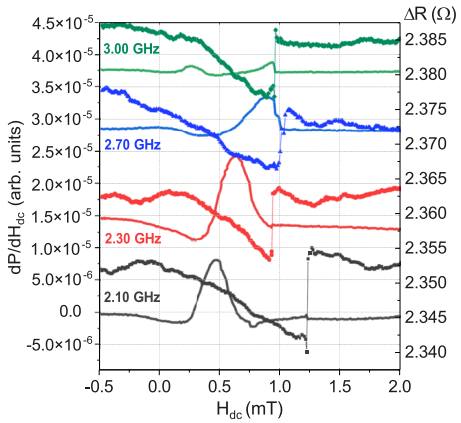

FIG. 4. Simultaneous FMR (line) and AMR measurements (line and symbols) for selected h_{RF} frequencies with the initial magnetization state saturated in a negative direction.

which the resonance is detected is lower than the depinning field. For higher fields, the FMR signal disappears. For the two measurements at 2.70 and 3.00 GHz, the interval of fields where the DW resonance is present overlaps with the sudden resistive transition marking the depinning field of the DW. At that precise field, the resonant peak ends abruptly, which evidences that the narrowband peak is associated with the presence of the DW shown in Fig. 3(a).

We conducted some simulations using Mumax 3 software, aiming to understand the unusual resonant behavior of the DW. With our resources, a simulation using the experimental dimensions implies prohibitive computational time. Therefore, we used a slightly smaller geometry like the one shown in Fig. 5(a), which is still very costly in terms of computation time. The cell size used in the simulation was $4 \times 4 \times 16$ nm^3, with only one cell size in the thickness of the strip. The magnetization and exchange stiffness used in the simulation were $M_s = 8.6 \times 10^5$ A/m and $A_{ex} = 13 \times 10^{-12}$. The simulation is initiated with a transversal wall like the one shown in Fig. 5(a). The DW quickly relaxes to a more complex wall like the one shown in Fig. 5(b), with a structure that does not resemble the experimental DW shown in Fig. 3(a). In the simulation, we have not managed to stabilize a DW like the one shown in Fig. 3(a), not even by locating scattered defects along the width of the strip. It is important to note that, if the experimental transversal DW shown in Fig. 3(a) had changed its structure during our measurements, we would have detected a sudden change in the AMR resistance, but this was not the case. Therefore, we realize that we are very likely not simulating the same DW that we are measuring in the experiment. We do not know the reason why the experimental transversal DW is so stable. Our guess is that a long crystalline boundary may run all across the stripe, fixing the shape of the DW.

In the simulation, we computed the resonant behavior for some values of H_{dc} in the presence of an RF field along the y axis of amplitude 60 μT. The DW undergoes a small oscillation, as shown in the snapshots in Figs. 5(b)–5(d). The structure of the DW is almost unaltered during the oscillation. The response of the DW to the RF field is monitored by the variation of the average magnetization in the y axis, Δm_y, which oscillates following the RF field as shown in Fig. 5(e). For three different values of H_{dc} and several frequencies of the RF field, we extracted the maximum amplitude of the oscillation. The results are shown in Fig. 5(f). The oscillation of the DW

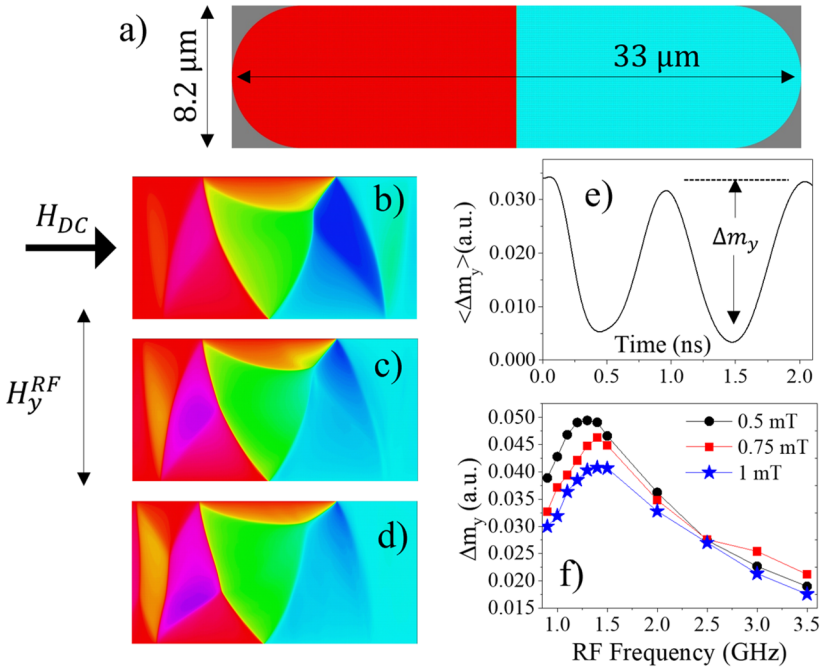

FIG. 5. (a) Initial configuration of the simulation with a transversal DW. The DW, for any field, adopts a shape similar to the one shown in (b), and it oscillates slightly under the action of the RF field as shown in (b)–(d). The average y-component of the magnetization in the DW oscillates under the action of the RF field (e). The amplitude of this oscillation changes with the frequency of the RF field, as shown in (f) for three different DC fields, 0.5, 0.75, and 1 mT.

is at its maximum around 1.4 GHz for all the fields, and although it increases slightly with H_{dc}, the resonant behavior of the simulated DW does not resemble the experimental results. A dedicated theoretical study, using sufficient computing power, is required to understand the peculiar resonant behavior characterized experimentally. Some aspects of the simulation need to be improved, such as the shape of the DW, the number of cells in the thickness, and the size of the strip, so the DW has a negligible interaction with the edges of the strip.

IV. CONCLUSION

To summarize, the ferromagnetic resonance of a permalloy microstrip has been measured at a range of frequencies between 2.0 and 3.5 GHz. Strip resonance peaks were observed for RF frequencies between 2.0 and 3.5 GHz in an interval of applied magnetic fields from −10 to 10 mT. One additional peak was observed for an interval of frequencies between 2.0 and 2.8 GHz. This additional peak is only present for external fields between 0.3 and 1 mT, and its characteristic frequency vs field behavior contrasts with the Kittel-type behavior characteristic of the strip resonance. Throughout magneto-optical Kerr effect microscopy and parallel magnetoresistance measurements, we could associate this narrowband peak with the presence of a large DW in the strip. The slope of the frequency vs field plot associated with the DW resonance is very large, 1.38 GHz/mT. This value and the excellent linearity of the behavior will allow the design of highly tunable RF oscillators and/or magnetic field sensing devices based on the resonance of large magnetic domain walls pinned at weak defects.

ACKNOWLEDGMENTS

This work has been partially funded by MCIN/AEI/10.13039/501100011033 through Project Nos. PID2020-117024GB-C42, PID2020-117024GB-C43, PID2020-117024GB-C44, and TED2021-130957B-C52, and by the European Union through Project No. H2020-2020-FETOPEN k-NET-899646. IMDEA Nanociencia acknowledges support from the Severo Ochoa Program for Centers of Excellence in R&D (Grant No. CEX2020-001039-S). Sandra Ruiz-Gómez acknowledges the support of the Alexander von Humboldt Foundation and the European Union under the Marie Skłodowska-Curie Grant Agreement No. 101061612.

AUTHOR DECLARATIONS

Conflict of Interest

The authors have no conflicts to disclose.

Author Contributions

Laura Fernández García: Conceptualization (equal); Data curation (equal); Formal analysis (equal); Methodology (equal); Writing – original draft (equal); Writing – review & editing (equal). **Sandra Ruiz-Gómez**: Conceptualization (equal); Methodology (equal); Supervision (equal); Writing – original draft (equal); Writing – review & editing (equal). **Rubén Guerrero**: Conceptualization

(equal); Methodology (equal); Writing – review & editing (equal). **Rodrigo Guedas**: Software (equal); Writing – review & editing (equal). **Claudio Aroca**: Methodology (equal); Validation (equal). **Lucas Perez**: Conceptualization (equal); Methodology (equal); Supervision (equal); Writing – review & editing (equal). **José L. Prieto**: Conceptualization (equal); Supervision (equal); Writing – original draft (equal); Writing – review & editing (equal). **Manuel Muñoz**: Conceptualization (equal); Data curation (equal); Formal analysis (equal); Methodology (equal); Project administration (equal); Resources (equal); Supervision (equal); Writing – original draft (equal); Writing – review & editing (equal).

DATA AVAILABILITY

The data that support the findings of this study are available from the corresponding author upon reasonable request.

REFERENCES

[1] S. A. Siddiqui, S. Dutta, A. Tang, L. Liu, C. A. Ross, and M. A. Baldo, "Magnetic domain wall based synaptic and activation function generator for neuromorphic accelerators," Nano Lett. **20**(2), 1033 (2020).

[2] F. Riente, G. Turvani, M. Vacca, and M. Graziano, "Parallel computation in the racetrack memory," IEEE Trans. Emerging Top. Comput. **10**(2), 1216 (2022).

[3] A. Barman *et al.*, "The 2021 magnonics roadmap," J. Phys.: Condens. Matter **33**, 413001 (2021).

[4] J. Grollier, M. V. Costache, C. H. van der Wal, and B. J. van Wees, "Microwave spectroscopy on magnetization reversal dynamics of nanomagnets with electronic detection," J. Appl. Phys. **100**, 024316 (2006).

[5] M. Hayashi, Y. K. Takahashi, and S. Mitani, "Microwave assisted resonant domain wall nucleation in permalloy nanowires," Appl. Phys. Lett. **101**, 172406 (2012).

[6] E. Saitoh, H. Miyajima, T. Yamaoka, and G. Tatara, "Current-induced resonance and mass determination of a single magnetic domain wall," Nature **432**, 203 (2004).

[7] L. Bocklage, B. Krüger, R. Eiselt, M. Bolte, P. Fischer, and G. Meier, "Time-resolved imaging of current-induced domain-wall oscillations," Phys. Rev. B **78**, 180405(R) (2008).

[8] S. Woo, T. Delaney, and G. S. D. Beach, "Magnetic domain wall depinning assisted by spin wave bursts," Nat. Phys. **13**, 448 (2017).

[9] R. B. Holländer, C. Müller, J. Schmalz, M. Gerken, and J. McCord, "Magnetic domain walls as broadband spin wave and elastic magnetisation wave emitters," Sci. Rep. **8**, 13871 (2018).

[10] K. Wagner, A. Kákay, K. Schultheiss, A. Henschke, T. Sebastian, and H. Schultheiss, "Magnetic domain walls as reconfigurable spin-wave nanochannels," Nat. Nanotechnol. **11**, 432 (2016).

[11] N. Sato, K. Schultheiss, L. Körber, N. Puwenberg, T. Mühl, A. A. Awad, S. S. P. K. Arekapudi, O. Hellwig, J. Fassbender, and H. Schultheiss, "Domain wall based spin-Hall nano-oscillators," Phys. Rev. Lett. **123**, 057204 (2019).

[12] A. Bisig, L. Heyne, O. Boulle, and M. Kläui, "Tunable steady-state domain wall oscillator with perpendicular magnetic anisotropy," Appl. Phys. Lett. **95**, 162504 (2009).

[13] S. Sharma *et al.*, "Proposal for a domain wall nano-oscillator driven by non-uniform spin currents," Sci. Rep. **5**, 14647 (2015).

[14] E. Martinez, L. Torres, and L. Lopez-Diaz, "Oscillator based on pinned domain walls driven by direct current," Phys. Rev. B **83**, 174444 (2011).

[15] J. H. Franken, R. Lavrijsen, J. T. Kohlhepp, H. J. M. Swagten, and B. Koopmans, "Tunable magnetic domain wall oscillator at an anisotropy boundary," Appl. Phys. Lett. **98**, 102512 (2011).

[16] C. W. Sandweg, S. J. Hermsdoerfer, H. Schultheiss, S. Schäfer, B. Leven, and B. Hillebrands, "Modification of the thermal spin-wave spectrum in a $Ni_{81}Fe_{19}$ stripe by a domain wall," J. Phys. D: Appl. Phys. **41**, 164008 (2008).

[17] S. Lepadatu, O. Wessely, A. Vanhaverbeke, R. Allenspach, A. Potenza, H. Marchetto, T. R. Charlton, S. Langridge, S. S. Dhesi, and C. H. Marrows, "Domain-wall spin-torque resonators for frequency-selective operation," Phys. Rev. B **81**, 060402(R) (2010).

[18] S. Lepadatu, J. S. Claydon, D. Ciudad, C. J. Kinane, S. Langridge, S. S. Dhesi, and C. H. Marrows, "Tuning of current-induced domain wall resonance frequency using Gd doping," Appl. Phys. Lett. **97**, 072507 (2010).

[19] P. J. Metaxas, M. Albert, S. Lequeux, V. Cros, J. Grollier, P. Bortolotti, A. Anane, and H. Fangohr, "Resonant translational, breathing, and twisting modes of transverse magnetic domain walls pinned at notches," Phys. Rev. B **93**, 054414 (2016).

[20] X. Wang, G. Guo, G. Zhang, Y. Nie, Q. Xia, and Z. Li, "Spin-transfer torque induced domain wall ferromagnetic resonance in nanostrips," J. Magn. Magn. Mater. **332**, 56 (2013).

[21] D. Bedau, M. Klaüi, S. Krzyk, U. Rüdiger, G. Faini, and L. Vila, "Detection of current-induced resonance of geometrically confined domain walls," Phys. Rev. Lett. **99**, 146601 (2007).

[22] Q. Mistral, M. van Kampen, G. Hrkac, J. V. Kim, T. Devolder, P. Crozat, C. Chappert, L. Lagae, and T. Schrefl, "Current-driven vortex oscillations in metallic nanocontacts," Phys. Rev. Lett. **100**, 257201 (2008).

[23] V. Novosad, F. Y. Fradin, P. E. Roy, K. S. Buchanan, K. Y. Guslienko, and S. D. Bader, "Magnetic vortex resonance in patterned ferromagnetic dots," Phys. Rev. B **72**, 024455 (2005).

[24] M. Hayashi, L. Thomas, Y. B. Bazaliy, C. Rettner, R. Moriya, X. Jiang, and S. S. P. Parkin, "Influence of current on field-driven domain wall motion in permalloy nanowires from time resolved measurements of anisotropic magnetoresistance," Phys. Rev. Lett. **96**, 197207 (2006).

[25] M. Hayashi, L. Thomas, C. Rettner, R. Moriya, and S. S. P. Parkin, "Direct observation of the coherent precession of magnetic domain walls propagating along permalloy nanowires," Nat. Phys. **3**, 21 (2007).

[26] J. Akerman, M. Muñoz, M. Maicas, and J. L. Prieto, "Stochastic nature of the domain wall depinning in permalloy magnetic nanowires," Phys. Rev. B **82**(6), 064426 (2010).